SEASONAL AND INTERANNUAL VARIABILITY OF SEA SURFACE CHLOROPHYLL CONCENTRATION IN THE COAST OF SRI LANKA

Gang Pan [1], Tilak P D Gamage [2], Dongxiao Wang [1]
[1]State Key Laboratory of Tropical Oceanography, South China Sea Institute of Oceanology, Chinese Academy of Sciences, China
Email: gpan@scsio.ac.cn
[2]Fishery and Marine Science and Technology, University of Ruhuna, Sri Lanka

KEY WORDS: Chlorophyll concentration; Remote Sensing; Variability; Sri Lanka

ABSTRACT: Many Indian Ocean fisheries are closely tied to eddy and upwelling variability. During the Southwest Monsoon, increased chlorophyll concentrations were observed from Moderate Resolution Imaging Spectrometer (MODIS) imagery along the southern coast of Sri Lanka. These phytoplankton bloom are associated with high primary productivity and have been attributed to coastal upwelling. Chlorophyll concentrations appeared low during the Northeast monsoon, but feeding aggregations of blue whales (*Balaenoptera musculus*) along the southern coast indicated evidence of high productivity. This meant that upwelling along the southern coast was prevalent throughout the year, instead of being limited to the Southwest Monsoon as previously thought. This study explored elements of the dynamics of the surface circulation and coastal upwelling in the waters around Sri Lanka using satellite imagery and in-situ observations. Quantifying these processes will be informative in predicting how these wake eddies and the upwelling associated with them might change in the future and, in particular, how they will respond to climate change and global warming.

1. INTRODUCTION

Sri Lanka is an island state lying between latitudes 5° 30' and 10° 00' North and longitudes 70° 30' and 82° 00' East in the Indian Ocean, bounded on the west by the Arabian Sea and the Gulf of Mannar and on the east by the Bay of Bengal. It has a coast line 1760 km long and a land area of 65 610 km^2. With the declaration of an Exclusive Economic Zone (EEZ), extending up to 200 miles, 436 000 km^2 of ocean have come under national jurisdiction, thus giving Sri Lanka a high water to land ratio.

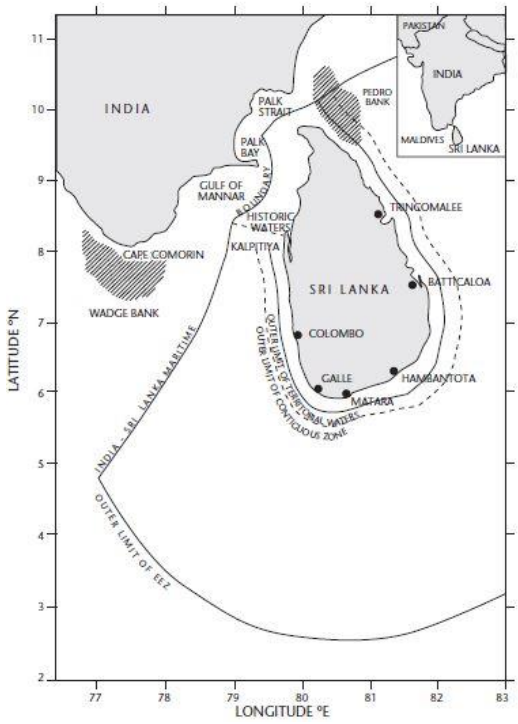

Fig. 1 Map of Sri Lanka Marine waters. (Source: Coastal Conservation Department)

Fisheries sector is playing a major role by contributing to food security and ensuring the nutrition of the population of Sri Lanka by contributing to nearly 2% of the GDP. In addition to that it plays a major role of the foreign exchange earnings in the country. Therefore with the facilities provided by the government and international non-government organizations, fishery sector is well in progress by providing economic and social wellbeing for

the people of the country.
In an oceanographic sense, the location of Sri Lanka is unique, with its offshore waters transporting water with different properties through reversing ocean currents driven by monsoon winds. The northern Indian Ocean is characterised by bi-annually reversing monsoon winds resulting from the seasonal differential heating and cooling of the continental land mass and the ocean. The Southwest (SW) monsoon generally operates between June and October, and the Northeast (NE) monsoon operates from December through April (Tomczak and Godfrey, 2003). The transition periods are termed the first inter-monsoon (May) and the second inter-monsoon (November). During the SW monsoon, the Southwest Monsoon Current (SMC) flows from west to east, transporting higher salinity water from the Arabian Sea, whilst during the NE monsoon, the currents reverse in direction, with the Northeast Monsoon Current (NMC) transporting lower salinity water originating from the Bay of Bengal from east to west (Schott and McCreary, 2001). During the SW monsoon, increased chlorophyll concentrations (> 5 mg m^{-3}) have been recorded around Sri Lanka, particularly along the southern coast (Vinayachandran et al., 2004), which appears to be a major upwelling region.
The continuity, global coverage, and high temporal and spatial resolution of satellite data make it an important tool for monitoring and characterizing marine ecosystems. Although satellites do not observe fish stocks directly, measurements such as sea-surface temperature (SST), sea-surface height (SSH), ocean color, ocean winds and sea ice, characterize critical habitat that influences marine resources. Most of the spatial features that are important to ecosystems, i.e. ocean fronts, eddies, convergence zones, river plumes and coastal regions, cannot be adequately resolved without satellite data. Chlorophyll is the only biological component of the marine ecosystem accessible to remote sensing (via ocean color), and as such provides a key metric for assessing the health and productivity of marine ecosystems on a global scale.
During the Southwest Monsoon, increased chlorophyll concentrations were observed from Moderate Resolution Imaging Spectrometer (MODIS) imagery along the southern coast of Sri Lanka. These phytoplankton bloom are associated with high primary productivity and have been attributed to coastal upwelling. Chlorophyll concentrations appeared low during the Northeast monsoon, but feeding aggregations of blue whales (*Balaenoptera musculus*) along the southern coast indicated evidence of high productivity. This meant that upwelling along the southern coast was prevalent throughout the year, instead of being limited to the Southwest Monsoon as previously thought. This study explored elements of the dynamics of the surface circulation and coastal upwelling in the waters around Sri Lanka using satellite imagery and in-situ observations.

2. DATA AND METHODS

Because the great area of the world's oceans makes it impossible to equip enough research vessels to study more than a small area of one ocean at one time, and because what happens in any one area of an ocean is dependent on processes at work in other parts of the world's oceans, oceanographers need the ability to study the oceans as a total system. Oceanographers are using remote sensing via satellites with specialized sensors and measuring devices to provide total ocean surveillance and data on a global scale. Many geophysical parameters can be derived from the satellite remote sensing data. Such as, sea surface temperature, chlorophyll concentration, sea surface salinity, sea surface height anomaly, sea wind, and rainfall etc.
The great advantage of remotely sensed images is that they show considerable environmental detail while also providing the widest possible context. The monitoring of global change will be of major scientific importance in the next several decades. New satellites and new programs mean vast amounts of new data being collected. These data and their interpretation will help us to find important pieces of the puzzle that oceanographers and other Earth scientists face as they work to develop a better understanding of the linkages between the ocean and other Earth systems.

3. RESULTS

3.1 Chlorophyll concentration

Chlorophyll is the material that allows algae cells to convert sunlight into energy, thus enabling them to grow, which is a good indicator of overall ocean health. Chlorophyll concentration is a proxy for phytoplankton productivity, and can be derived from satellite remote sensing data based on the relationship to the blue-to-green ratio of water-leaving radiances. Since the Coastal Zone Color Scanner (CZCS) was launched in 1978, satellite ocean color data have been successfully used to monitor phytoplankton in surface waters. By measuring chlorophyll can identify areas rich in nutrients and monitor such processes such as upwelling. As the surface water moves offshore, cold, nutrient-rich water upwells from below to replace it. This upwelling provides nutrients needed for the growth of marine phytoplankton which, along with larger seaweeds, in turn nourish the incredible diversity of creatures found along the coast.
Satellite-based ocean color observations provide a global picture of life in the world's oceans. Sensors such as CZCS can "see" the effects of this upwelling-related productivity because the chlorophyll-bearing phytoplankton reflect predominantly green light back into space as opposed to the water itself which reflects predominantly blue wavelengths back to space. The Sea-viewing Wide Field-of-view Sensor (SeaWiFS) was a follow-on to CZCS, launched in 1997. The MODIS/Aqua instrument currently provides ocean color data.

By recording images over a period of years, scientists also gained a better understanding of how the phytoplankton biomass changed over time; for instance, red tide blooms could be observed when they grew. Ocean color measurements are also of interest because phytoplankton removes carbon dioxide from the sea water during photosynthesis, and so forms an important part of the global carbon cycle.

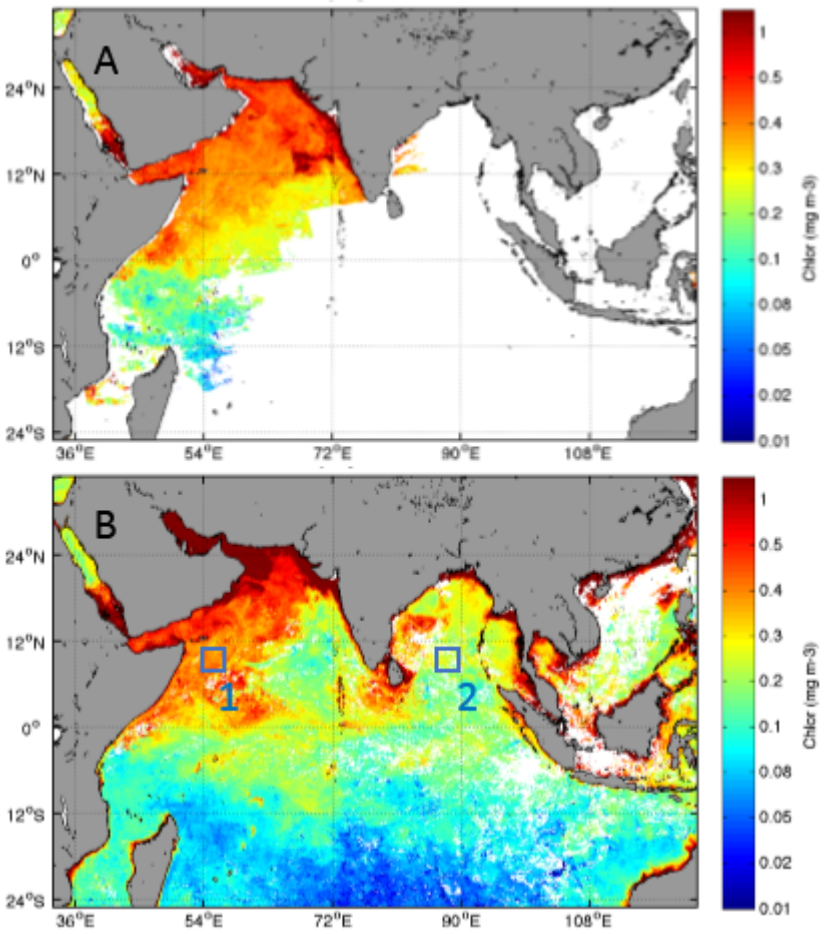

Fig. 2. Monthly averaged Chlorophyll concentration in December in different year. (A) Chl derived from CZCS data in 1978, and (B) Chl derived from MODIS/Aqua in 2014.

The earliest monthly averaged Chlorophyll concentration (Dec 1978, Fig. 4A) and recent monthly Chlorophyll (Dec 2014, Fig. 4B) were present. By comparing the two different date Chl data in the same month, there are much higher Chl in Northwest Arabian Sea and the coastal area than the earlier. The 4km resolution monthly CZCS and MODIS/Aqua data were obtained from NASA (http://oceancolor.gsfc.nasa.gov/cgi/l3).

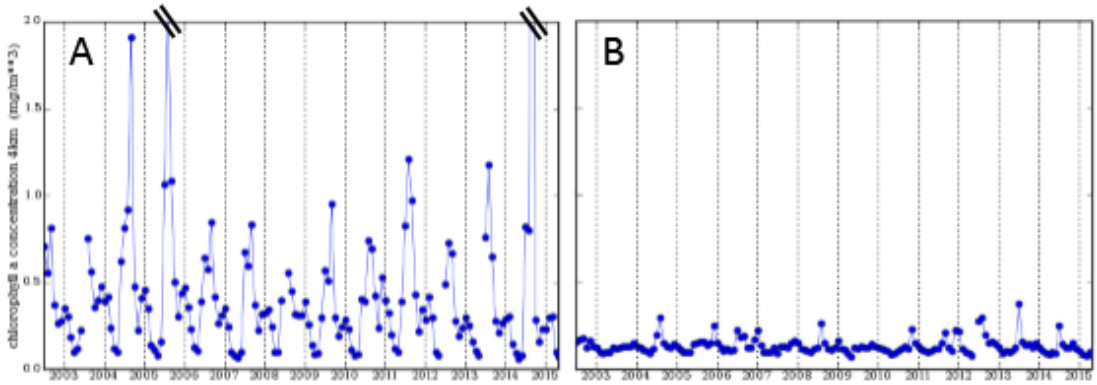

Fig. 3. Area-averaged time series MODIS/Aqua Chlorophyll 4km resolution during Jul 2002 – May 2015. Region 54-57E, 9-12N (A), and region 87-90E, 9-12N (B), which corresponding to the blue boxes 1 and 2 in Fig. 4B, respectively.

Same as the SST data, Chl data also can be used for time series analysis. Two area-averaged time series Chl data

were present during Jul 2002 – May 2015 (Fig. 5). The monthly averaged Chl data derived from the same sensor MODIS/Aqua, with 4km resolution. During this time, the Chlorophyll concentration of box 1 (Fig. 5A) was higher than box 2 (Fig. 5B), with high variability.

3.2 Sea surface temperature (SST)

SST is the temperature of the top millimeter of the ocean's surface. SST is an important geophysical parameter, providing the boundary condition used in the estimation of heat flux at the air-sea interface. On the global scale this is important for climate modeling, study of the earth's heat balance, and insight into atmospheric and oceanic circulation patterns and anomalies (such as El Niño). On a more local scale, SST can be used operationally to assess eddies, fronts and upwelling for marine navigation and to track biological productivity.

In the past, SST could only be measured by ships and buoys, whose ranges were limited. Satellite technology has improved upon our ability to measure SST by allowing frequent and global coverage. Methods for determining SST from satellite remote sensing include thermal infrared and passive microwave radiometry.

Thermal infrared SST measurements have a long heritage (more than 30 years). They are derived from radiometric observations at wavelengths of ~3.7 µm and/or near 10 µm. Both bands are sensitive to the presence of clouds and scattering by aerosols and atmospheric water vapor. For this reason, thermal infrared measurements of SST first require atmospheric correction of the retrieved signal and can only be made for cloud-free pixels. Thus, maps of SST compiled from thermal infrared measurements are often weekly or monthly composites which allow enough time to capture cloud-free pixels over a region. Thermal infrared instruments that have been used for deriving SST from Advanced Very High Resolution Radiometer (AVHRR) on NOAA Polar-orbiting Operational Environmental Satellites (POES), with the first global composites occurring during 1970 (Krishna et al., 1972). Since September 1981, satellites have been increasingly utilized to measure SST and have allowed its spatial and temporal variation to be viewed more fully (Fig. 2). After that, Along-Track Scanning Radiometer (ATSR) aboard the European Remote Sensing Satellite (ERS-2), the Geostationary Operational Environmental Satellite (GOES) Imager, Moderate Resolution Imaging Spectroradiometer (MODIS) aboard NASA Terra and Aqua satellites, and Visible Infrared Imaging Radiometer Suite (VIIRS) aboard Suomi National Polar-orbiting Partnership (Suomi NPP) were followed.

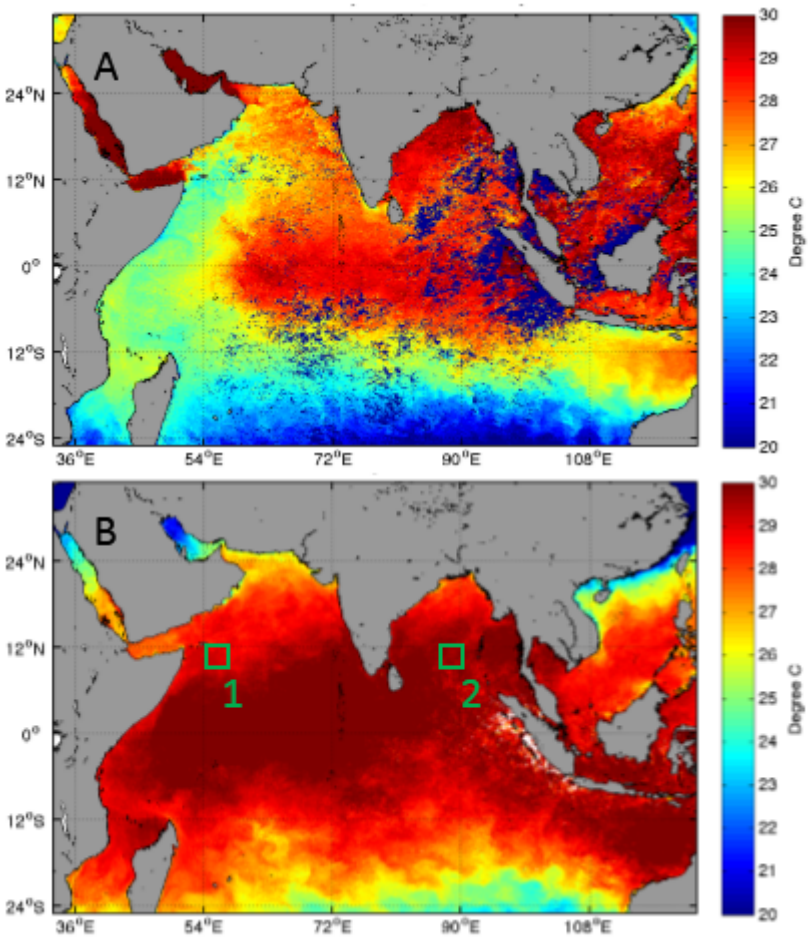

Fig. 4. Monthly averaged SST data in different time. (A) SST derived from the AVHRR sensor onboard the satellite NOAA-7 in September 1981, and (B) SST derived from the MODIS sensor onboard the satellite Aqua in April 2015.

The satellite-measured SST provided both a synoptic view of the ocean and a high frequency of repeat views. Monthly averaged SST data were present in different time (Fig. 2). The earlier SST (Fig. 2A) derived from the AVHRR Pathfinder Version 5.1 (PFV51) data set in September 1981, which was computed using an entirely modernized system, based on SeaDAS and incorporating several key changes over the older Pathfinder datasets (ftp://ftp.nodc.noaa.gov/pub/data.nodc/pathfinder). The newer SST (Fig. 2B) derived from the MODIS sensor onboard the satellite Aqua in April 2015. MODIS SST data were downloaded from NASA's ocean color website (http://oceancolor.gsfc.nasa.gov/cgi/l3). According to the color map, the temperature in April 2015 was higher than in September 1981 in the same area.

Due to the long heritage of the thermal infrared SST data (more than 30 years), those can be used for time series analysis. Two area-averaged time series SST data were present during Jul 2002 – May 2015 (Fig. 3). The monthly averaged SST data derived from the same sensor MODIS/Aqua, with 4km resolution. During this time, the temperature of box 2 (Fig. 3B) was higher than box 1 (Fig. 3A), which was the same longitude. The temperature of box 1 has more variable than box 2. In fact, time resolution of SST was much shorter than 1 month. There are many weekly averaged, 3-day averaged, and then daily SST data. Using these high frequency SST data, we can analysis the seasonal change, rather than interannual.

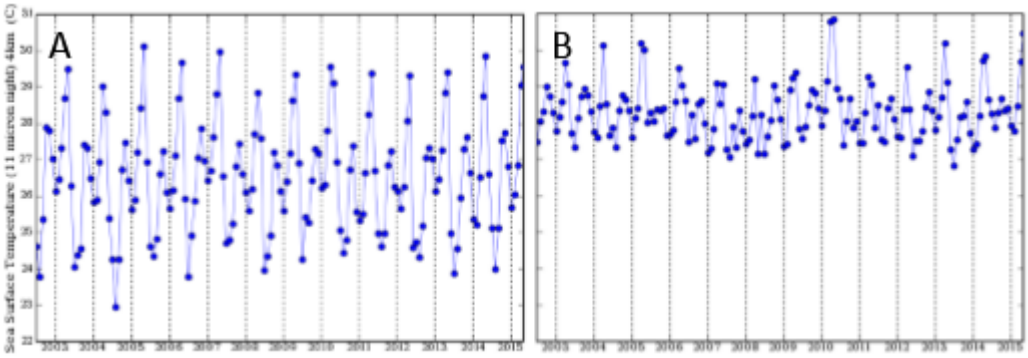

Fig. 5. Area-averaged time series MODIS/Aqua night SST 4km resolution during Jul 2002 – May 2015. Region 54-57E, 9-12N (A), and region 87-90E, 9-12N (B), which corresponding to the green boxes 1 and 2 in Fig. 2B, respectively.

3.3 Sea surface salinity

Sea surface salinity (SSS) is a key component of Earth's climate that is linked to the cycling of freshwater around our planet and that influences ocean circulation, which reflects the balance between precipitation and evaporation. Differences in salinity play a major role in moving seawater around the globe. Salinity and temperature drive circulation by controlling the density of seawater, which is crucial to moving heat around our planet.

When combined with data from other satellite sensors, salinity remotely sensed data provide a clearer picture of how the ocean works, how it is linked to climate - including short-term events like El Niño and La Niña - and how it may respond to climate change. By measuring changes in SSS caused by these processes, as well as changes caused by melting ice and river runoff, salinity sensor provides important new information about how Earth's freshwater moves between the ocean and atmosphere and around the globe.

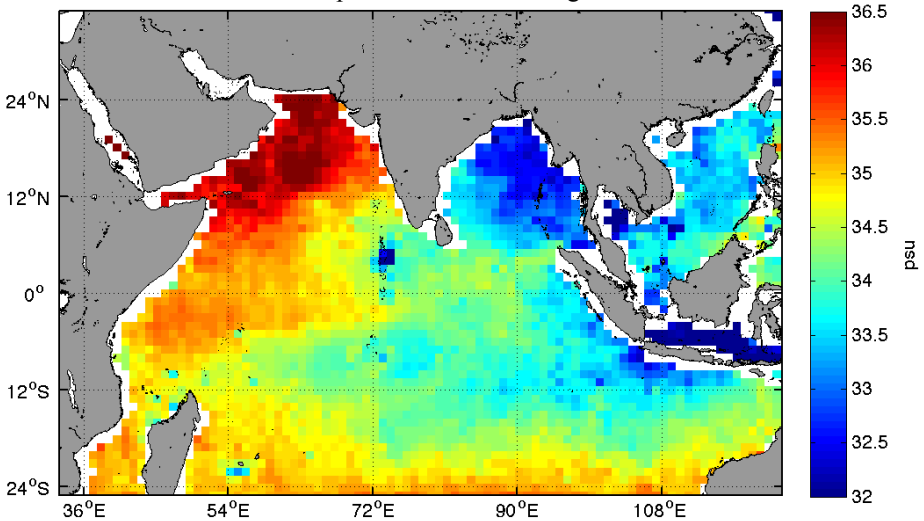

Fig. 6. Monthly SSS in Apr 2015. Data from http://oceancolor.gsfc.nasa.gov/cgi/l3

Aquarius sensor onboard the SAC-D spacecraft measure SSS by using radiometers to detect changes in the oceans microwave thermal emissions frequencies due to salinity. Aquarius' three radiometers have antenna reflectors 2.5 meters in diameter that are able to scan a 390 km wide swath of the ocean's surface collectively. The radiometers on Aquarius are the most accurate ever and are able to sense at a frequency of 1.4 GHz. The observatory was successfully launched on June 10, 2011 to a 657 km sun-synchronous orbit. Project Aquarius attempts to monitor SSS with an accuracy of 0.1 psu (practical salinity unit). SMOS (Soil Moisture and Ocean Salinity) mission operated by the European Space Agency exploits an innovative instrument designed as a 2D interferometer acquiring globally brightness temperatures at L-band (1.4GHz) to retrieve salinity fields over the oceans.
The map (Fig. 6) shows important regional features, including a sharp contrast between the arid, high-salinity Arabian Sea west of the Indian subcontinent, and the low-salinity Bay of Bengal to the east, which is dominated by the Ganges River and south Asia monsoon rains. Its rich tapestry of global salinity patterns demonstrates Aquarius' ability to resolve large-scale salinity distribution features clearly and with sharp contrast.

3.4 Sea surface height anomaly

Sea surface height (SSH, or sea level) is the height of the ocean's surface. SSH is of interest to scientists because it reveals information about how much heat is stored in the ocean. Warm water is less dense than cold water, so higher areas tend to be warmer than lower areas. Across the seasonal cycle changes in patterns of warming, cooling and surface wind forcing affect circulation and influence SSH.
When the ocean contains a sea surface height gradient this creates a jet or current, such as the Antarctic Circumpolar Current. This current as part of a baroclinically unstable system meanders and creates eddies. Eddies which are between about 10 and 500 km in diameter, and persist for periods of days to months are known in oceanography as mesoscale eddies. Mesoscale eddies have been observed in many of major ocean currents, including the Gulf Stream, the Agulhas Current, the Kuroshio Current, and the Antarctic Circumpolar Current, amongst others.

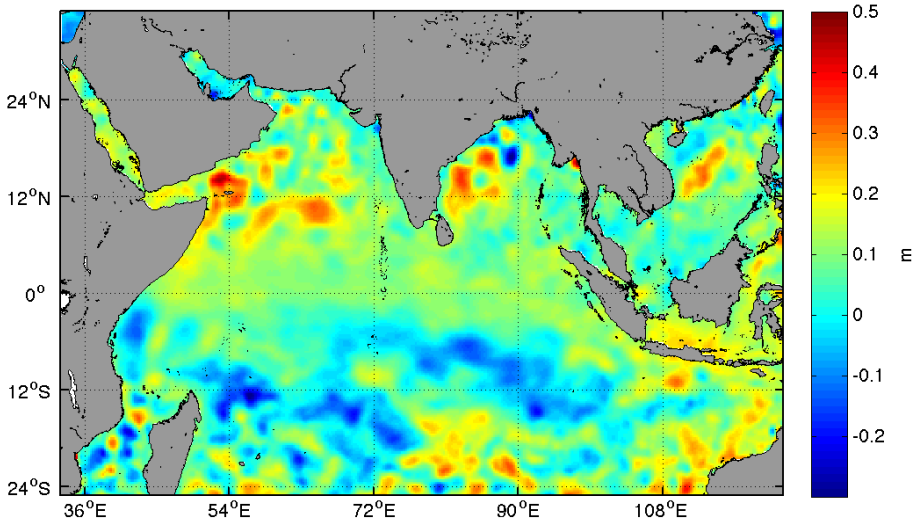

Fig. 7. A snapshot of sea level anomaly on Apr 29, 2013. The spatial resolution is 1/4°x1/4°. Data from: ftp://ftpsedr.cls.fr/pub/oceano/AVISO/SSH/duacs/global/dt/upd /msla/merged/h/

Variations in SSH can be measured by satellite altimetry (e.g. Jason, TOPEX/Poseidon). SSH anomalies (or Sea Level Anomalies, SLA) are computed from the difference of the instantaneous SSH - a temporal reference. This temporal reference can be a mean profile in the case of repeat track. In the Duacs 2014 version (v15.0), the reference period of the SLA is based on a 20-year [1993, 2012] period. Gridded maps of SLA (Fig. 7) merged from TOPEX/ Poseidon, Jason and ERS-1/2 created by SSALTO/DUACS and distributed by AVISO (Archiving, Validation and Interpretation of Satellite Oceanographic data). These data are used in ocean models to calculate the speed and direction of ocean currents and the amount and location of heat stored in the ocean, which in turn reveals global climate variations.

3.5 Sea wind

Accurate wind vector data aid in short-term weather forecasting, the issuing of timely weather warnings, and the gathering of general climatological data. The ocean surface wind vector can be measured from space using a polarimetric microwave radiometry.
The Quick Scatterometer (a SeaWinds instrument placed in orbit quickly) was launched in June 1999 and operated until November 2009. The primary mission of these SeaWinds scatterometers was to measure winds near the ocean surface. The SeaWinds instruments are the third in a series of NASA scatterometers that operate at Ku-band (i.e., a frequency near 14 GHz). The first Ku-Band scatterometer was flown on SeaSat in 1978. Eighteen years later, NSCAT was launched on Japan's Midori-I (ADEOS-I) spacecraft in August 1996. The Europeans also fly satellite

scatterometers, which operate at C-band (approx. 5 GHz). Two of these, named ASCAT, are currently operating. Scatterometers emit pulses of low-power microwave radiation and measure the power reflected back to its receiving antenna from the wind-roughened sea surface. Gravity and capillary waves on the sea surface caused by the wind reflect or backscatter power emitted from the scatterometer radar primarily by means of a Bragg resonance condition. QuikSCAT consists of an active microwave radar that infers surface winds from the roughness of the sea surface based on measurements of radar backscatter cross section. QuikSCAT uses a dual-beam, conically scanning antenna that samples the full range of azimuth angles during each antenna revolution (Ricciardulli et al., 2013). Wind speed and direction at a height of 10 meters over ice-free oceans are retrieved from backscattered scatterometer signals. Level 3 gridded data are distributed by Remote Sensing Systems at daily, 3-day and monthly resolution on a 0.25 degree grid (Fig. 8).

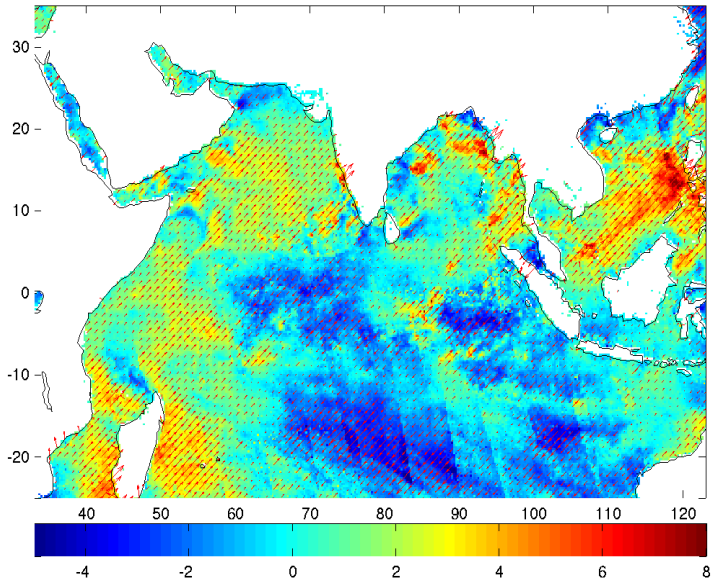

Fig.8. A snapshot of 29th week wind anomalies in autumn of 1999 (Day of year 199-205). The red arrows plotted on this image are wind vectors. These vectors indicate direction and intensity of the wind. The vectors point in the direction to which the wind is blowing and in this image, winds are primarily blowing from west to east. Intensity of the wind is conveyed through the size of the vector. The color filled regions indicate wind speed in knots and is color coded according to the legend at the bottom of the image.

3.6 Rainfall data

Rainfall intensity retrievals from space-borne sensors have been based mostly on passive sensors for about 30 years using visible, infrared and passive microwave wavelengths on geostationary and low Earth orbiting satellites. Since the launch of the Tropical Rainfall Measuring Mission (TRMM) in 1997 the first precipitation radar is operating in space. The availability of active precipitation detection from space has laid the groundwork for space-borne estimations from radar and radar + radiometer (Michaelides et al., 2009). The most widely known of the statistical-physical algorithms is the Goddard Profiling (GPROF) technique (Kummerow et al., 2001). GPROF retrieves the instantaneous rainfall and the rainfall vertical structure using the response functions for different channels peaking at different depths within the rain column. The algorithm is based upon a Bayesian approach that begins by establishing a large database of potential hydrometeor profiles and their computed brightness temperatures.

The TRMM Multi-Satellite Precipitation Analysis (TMPA; computed at monthly intervals as 3B43) combines the estimates generated by the TRMM and other satellites product and the CAMS global gridded rain gauge data, produced by NOAA's Climate Prediction Center and/or the global rain gauge product produced by the Global Precipitation Climatology Center. The output is precipitation (units: mm/hr) for 0.25x0.25 degree grid boxes for each month. The monthly rainfall during Feb 2015 was shown as follow (Fig. 9).

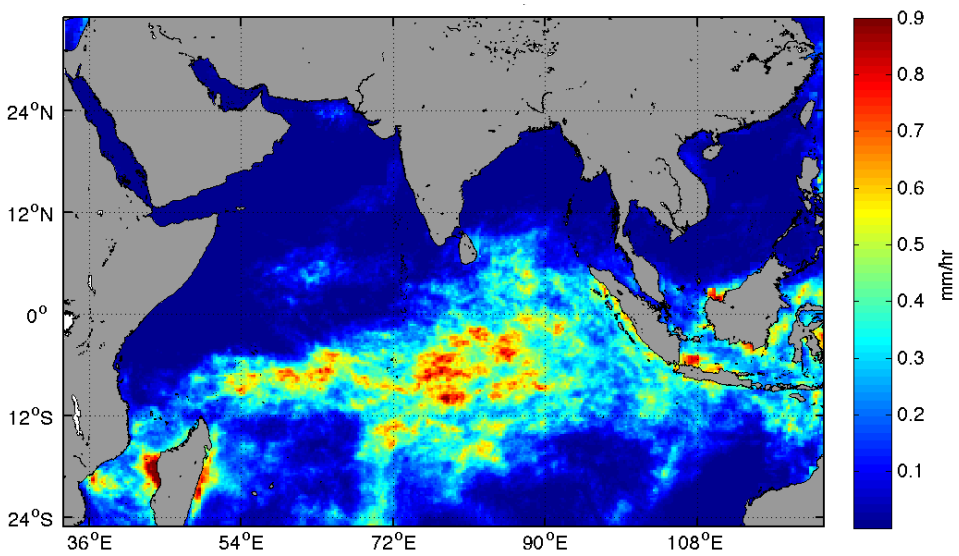

Fig. 9. Monthly rainfall during in Feb 2015, data from TRMM 3B43 product.

4. CONCLUSION

Satellite remote sensing technique was an important tool for fighting the environment and resource problem, which can acquire large area information at the same time. The available satellite data were summarized in here, such as, SST, chlorophyll concentration, SSS, SSHA, sea wind, rainfall and so on. Using these remote-sensed data, many marine physical phenomena were investigated, that is, Indian Ocean dipole was confirmed, phytoplankton bloom initiating was observed and clarified, at the same time, many extreme events also introduce the phytoplankton bloom, such as, tsunami and oil spill. In a word, remote sensing technology can play an important role in optimizing the allocation of resources and preventing the disaster. Quantifying these processes will be informative in predicting how these wake eddies and the upwelling associated with them might change in the future and, in particular, how they will respond to climate change and global warming.

ACKNOWLEDGEMENT

This study was supported through the China-Sri Lanka Joint Center for Education & Research, Chinese Academy of Sciences.

REFERENCES

Bentley, J (1993) Old World Encounters: Cross-Cultural Contacts and Exchanges in Pre-Modern Times. New York: Oxford University Press, 33.

Elisseeff V (2001) The Silk Roads: Highways of Culture and Commerce. UNESCO Publishing / Berghahn Books. ISBN 978-92-3-103652-1.

Kahru, M, Fiedler PC, Gille ST, Manzano M, Mitchell BG. (2007) Sea level anomalies control phytoplankton biomass in the Costa Rica Dome area. Geophysical Research Letters. 34

Krishna Rao, P., W. L. Smith, and R. Koffler (1972). Global Sea-Surface Temperature Distribution Determined From an Environmental Satellite. Monthly Weather Review 100 (1): 10–14.

Kummerow, C., Y. Hong, W.S. Olson, S. Yang, R.F. Adler, J. McCollum, R. Ferraro, G. Petty, D.-B. Shin, T.T. Wilheit (2001) The evolution of the Goddard Profiling Algorithm (GPROF) for rainfall estimation from passive microwave sensors J. Appl. Meteorol., 40, 1801–1820.

Levathes, L (1996). When China Ruled the Seas: The Treasure Fleet of the Dragon Throne, 1405–1433. New York: Oxford University Press. ISBN 9780195112078.

Michaelides, S., V. Levizzani, E. Anagnostou, P. Bauer, T. Kasparis, J.E. Lane (2009) Precipitation: Measurement, remote sensing, climatology and modeling, Atmospheric Research, 94, 4, 512-533.

Ricciardulli, Lucrezia & National Center for Atmospheric Research Staff (Eds). Last modified 20 Nov 2013. "The Climate Data Guide: QuikSCAT: near sea-surface wind speed and direction." Retrieved from https://climatedataguide.ucar.edu/climate-data/quikscat-near-sea-surface-wind-speed-and-direction.

Schott, F. A. and McCreary, Jr., J. P.: The monsoon circulation of the Indian Ocean, Prog. Oceanogr., 51, 1–123, 2001.

Tomczak, M. and Godfrey, J. S.: Regional oceanography: An introduction, 2 Edn., Pergamon, 2003.

Vinayachandran, P. N., Chauhan, P., Mohan, M., and Nayak, S.: Biological response of the sea around Sri Lanka to summer monsoon, Geophys. Res. Lett., 31, L01302, doi:10.1029/2003GL018533, 2004.